



Green synthesis, characterization, and antibacterial activity of gold nanoparticles

H. H. Esmael, R. N. Taha, N. S. Mohamed

Al-Nahrain University, Baghdad, Iraq

Article info

Received 04.02.2026

Received in revised form
04.03.2026

Accepted 27.03.2026

Clinical Laboratory
Science Branch, College
of Pharmacy, Al-Nahrain
University, Baghdad, Iraq.
E-mail:
dr.havraa.hashim@
nahrainuniv.edu.iq

Esmael, H. H., Taha, R. N., & Mohamed, N. S. (2026). Green synthesis, characterization, and antibacterial activity of gold nanoparticles. *Regulatory Mechanisms in Biosystems*, 17(2), e26050. doi:10.15421/0226050

Green synthesis of gold nanoparticles (AuNPs) offers an eco-friendly alternative to conventional chemical methods for biomedical applications. In this study, AuNPs were synthesized using an aqueous extract of *Syzygium aromaticum* (clove), where phytochemicals acted as reducing and stabilizing agents. The synthesized nanoparticles were characterized using UV-visible spectroscopy, X-ray diffraction (XRD), atomic force microscopy (AFM), and transmission electron microscopy (TEM). UV-vis analysis confirmed nanoparticle formation through a characteristic surface plasmon resonance band, while XRD revealed a face-centered cubic crystalline structure. AFM and TEM analyses showed predominantly spherical AuNPs with an average particle size of 15–20 nm. The antibacterial activity of clove-mediated AuNPs was evaluated against *Staphylococcus aureus*, *Escherichia coli*, and *Pseudomonas aeruginosa* using disc diffusion, MTT, and LDH assays. The results demonstrated a clear concentration-dependent antibacterial effect, with higher sensitivity observed for Gram-positive bacteria. Increased LDH release and reduced MTT activity indicated membrane damage and decreased bacterial viability, with promising applications.

Keywords: green synthesis; gold nanoparticles; *Syzygium aromaticum*; antibacterial activity; MTT assay; LDH assay.

Introduction

Nanotechnology has enabled the design and fabrication of materials at the nanoscale (1–100 nm), where unique physicochemical, optical, and electronic properties arise. Metal nanoparticles (MNPs), especially gold nanoparticles (AuNPs), are highly valued for their biocompatibility, chemical stability, ease of surface functionalization, and surface plasmon resonance (SPR), making them suitable for biomedical applications such as drug delivery, diagnostics, bioimaging, and antimicrobial therapy (Bindhu & Umadevi, 2014; Hadi & Ibrahim, 2024).

Conventional chemical and physical synthesis methods often involve toxic chemicals, hazardous solvents, and high energy consumption, which can leave residual contaminants and limit biocompatibility. Green synthesis offers a sustainable alternative, using plant extracts, microorganisms, or enzymes to reduce metal ions under mild and eco-friendly conditions. Plant-derived phytochemicals act as both reducing and stabilizing agents, controlling nanoparticle formation while enhancing biological activity (Hashem et al., 2022).

Clove (*Syzygium aromaticum*) is rich in eugenol, phenolics, and terpenoids, which can reduce Au^{3+} ions to metallic Au^0 and simultaneously stabilize the nanoparticles, producing monodispersed and bioactive AuNPs (Khalifa & Alkhoori, 2025). These clove-mediated AuNPs exhibit strong antibacterial activity against Gram-positive (*Staphylococcus aureus*) and Gram-negative bacteria (*Escherichia coli*, *Pseudomonas aeruginosa*) through membrane disruption, reactive oxygen species (ROS) generation, and enzyme inhibition, showing enhanced efficacy compared to plant extract or nanoparticles alone (Bano, 2019; Xu et al., 2023).

This study integrates green chemistry, nanotechnology, and plant-based therapeutics to develop stable, biocompatible AuNPs with potent antibacterial properties, offering a sustainable platform for medical and pharmaceutical applications, particularly in addressing bacterial infections and antibiotic resistance (Rai et al., 2009; Ahmed et al., 2016).

Materials and methods

Clove (*Syzygium aromaticum*) buds were thoroughly washed with distilled water to remove dust and impurities and then air-dried at room temperature to preserve their bioactive constituents. The dried buds were finely ground to increase the surface area for efficient extraction of phytochemicals. Ten grams of clove powder were mixed

with 100 mL of deionized water and heated at 80 °C for 15 min to facilitate the release of active compounds such as eugenol, phenolics, and terpenoids into the solution. The mixture was allowed to cool to room temperature and filtered through Whatman filter paper to obtain a clear aqueous extract. The extract was used immediately for nanoparticle synthesis or stored at 4 °C for short-term use (Hemlata et al., 2020; Hadi & Ibrahim, 2024).

A 1 mM solution of chloroauric acid (HAuCl_4) was prepared in deionized water as the gold precursor. The aqueous clove extract was added dropwise under constant magnetic stirring at room temperature to ensure uniform mixing and controlled nucleation of nanoparticles. Formation of gold nanoparticles was indicated by a visible color change from pale yellow to ruby red due to surface plasmon resonance (SPR). This change reflects the reduction of Au^{3+} ions to metallic Au^0 and stabilization by phytochemicals such as eugenol, phenolics, and terpenoids present in the clove extract (Rai et al., 2009; Dikshit et al., 2021; Hadi & Ibrahim, 2024; Muhammed et al., 2025). The reaction was continued until color stabilization confirmed successful synthesis of stable monodispersed AuNPs.

The antibacterial and cytotoxic effects of green-synthesized gold nanoparticles (AuNPs) prepared using *Syzygium aromaticum* extract were evaluated against *Staphylococcus aureus*, *Escherichia coli*, and *Pseudomonas aeruginosa*, commonly used as antimicrobial model organisms due to their clinical relevance and resistance potential (Rai et al., 2009; Ahmed et al., 2016). All strains were cultured in nutrient broth at 37 °C for 18–24 h prior to experimentation.

The lactate dehydrogenase (LDH) release assay was used to evaluate bacterial membrane integrity after treatment with clove-mediated AuNPs. Membrane disruption causes leakage of intracellular LDH into the extracellular medium, serving as an indicator of membrane damage (Ahmed et al., 2016; Hemlata et al., 2020).

Bacterial cultures adjusted to 0.5 McFarland standard were exposed to AuNP concentrations ranging from 5–100 $\mu\text{g}/\text{mL}$ and incubated at 37 °C for 24 h. Samples were centrifuged at 5000 rpm for 10 min, and LDH activity in the supernatant was measured at 490 nm using a microplate reader. Untreated cultures served as negative controls, while ethanol-treated cultures served as positive controls according to antimicrobial susceptibility standards (Clinical and Laboratory Standards Institute, 2022). Increased LDH release indicated AuNP-induced membrane damage and bactericidal activity (Slater et al., 1963).

The cytotoxic effect of clove-mediated AuNPs was evaluated using Vero cells (African green monkey kidney cells), a standard mam-

malian model for biocompatibility assessment. Cells were cultured in Dulbecco's Modified Eagle Medium (DMEM) supplemented with 10% fetal bovine serum (FBS) and 1% penicillin-streptomycin and maintained at 37 °C in a humidified incubator containing 5% CO₂.

LDH release assay was used to evaluate membrane integrity and cytotoxicity induced by AuNPs. Vero cells were seeded in 96-well plates at a density of 1×10^4 cells/well and incubated for 24 h to allow attachment. Cells were then treated with AuNP concentrations of 5, 10, 25, 50, and 100 µg/mL for 24 h. LDH activity was measured at 490 nm according to the manufacturer's protocol, and cytotoxicity percentage was calculated relative to maximum LDH release control (Akhtar et al., 2024).

The MTT assay was used to assess bacterial metabolic activity and viability following AuNP exposure. Viable bacterial cells reduce MTT into insoluble formazan crystals through respiratory enzyme activity (Slater et al., 1963).

Bacterial suspensions adjusted to 0.5 McFarland were treated with AuNPs and incubated at 37 °C for 24 h. MTT solution (0.5 mg/mL) was added and incubated for 2–4 h. Formazan crystals were dissolved using DMSO, and absorbance was measured at 570 nm. Reduced absorbance indicated decreased bacterial viability and antimicrobial activity of AuNPs.

Antibacterial activity of clove-mediated AuNPs was evaluated using the disc diffusion method against *S. aureus*, *E. coli*, and *P. aeruginosa* following antimicrobial susceptibility testing standards (Clinical and Laboratory Standards Institute, 2022).

Bacterial cultures standardized to 0.5 McFarland ($\sim 1 \times 10^8$ CFU/mL) were spread on nutrient agar plates. Sterile discs impregnated with AuNP concentrations (5–100 µg/mL) were placed on inoculated plates. Norfloxacin discs were used as positive controls, while blank discs served as negative controls. Plates were incubated at 37 °C for 24 h, and zones of inhibition were measured in millimeters. Experiments were performed in triplicate to evaluate dose-dependent antibacterial effects.

Results

UV-visible absorption spectroscopy is widely used to characterize the optical properties of gold nanoparticles (AuNPs). AuNPs exhibit a characteristic localized surface plasmon resonance (LSPR) band in the visible region (~500–600 nm), caused by collective oscillations of conduction electrons at the nanoparticle surface. The position and intensity of this band depend on particle size, shape, surface chemistry, and the surrounding medium, making UV-vis spectroscopy a key tool to confirm nanoparticle formation.

In green synthesis using plant extracts, phytochemicals such as flavonoids, polyphenols, and terpenoids act as reducing and stabilizing agents, converting Au³⁺ ions to Au⁰ and preventing aggregation. Successful synthesis is confirmed by the visible color change (from yellow to red/purple) and the appearance of the LSPR peak in the UV-vis spectrum (Gong et al., 2024). Unlike semiconductor nanoparticles, where the optical band gap is derived from Tauc plots, the optical response of AuNPs is dominated by plasmonic effects, providing information about particle morphology and surface environment.

The powder X-ray diffraction (XRD) pattern of the synthesized AuNPs shows peaks consistent with the standard face-centered cubic (fcc) structure of metallic gold (JCPDS card no. 04-0784). Diffraction peaks at 2θ values of approximately 38.2°, 44.4°, 64.6°, and 77.5° can be indexed to the (111), (200), (220), and (311) planes, respectively, confirming that the AuNPs are polycrystalline with a cubic phase (Iravani, 2011).

The sharpness and intensity of the diffraction peaks indicate good crystallinity, while the absence of additional peaks suggests the nanoparticles are pure. The XRD pattern also allows estimation of the average crystallite size using the Debye-Scherrer equation, typically in the range of 10–25 nm for biosynthesized AuNPs, depending on synthesis conditions and capping agents (Muddapur et al., 2022).

The formation of gold nanoparticles (AuNPs) was confirmed by UV-vis spectroscopy through the appearance of a characteristic surface plasmon resonance (SPR) band, indicating the successful reduc-

tion of Au³⁺ ions to metallic Au⁰ nanoparticles. The position and shape of the SPR band are consistent with nanosized gold particles synthesized via green methods (Iravani, 2011; Muddapur et al., 2022).

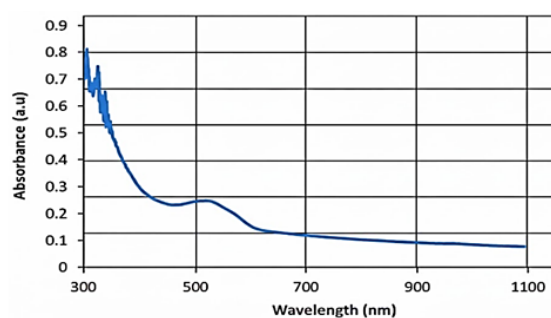


Fig. 1. UV-visible absorption spectrum of clove-mediated gold nanoparticles (AuNPs) showing the characteristic surface plasmon resonance band

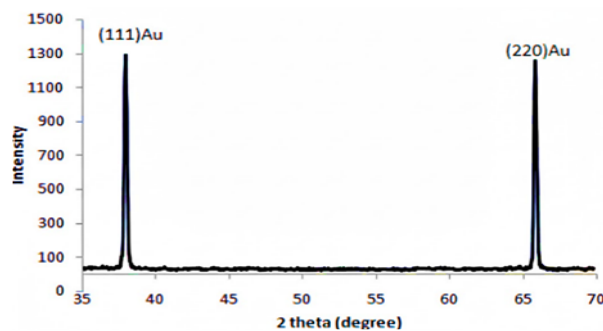


Fig. 2. XRD image of Au NPs

AFM analysis further supported these findings by revealing uniformly distributed AuNPs with predominantly quasi-spherical morphology. The 2D and 3D AFM images (Fig. 3) showed nanoscale height variations, with particle heights reaching approximately 15–16 nm, confirming nanoparticle formation. Minor agglomeration observed in the images is attributed to phytochemicals acting as natural reducing and capping agents during green synthesis (Muddapur et al., 2022; Gong et al., 2024). Overall, the AFM and UV-vis results collectively confirm the successful synthesis of stable gold nanoparticles suitable for biomedical applications.

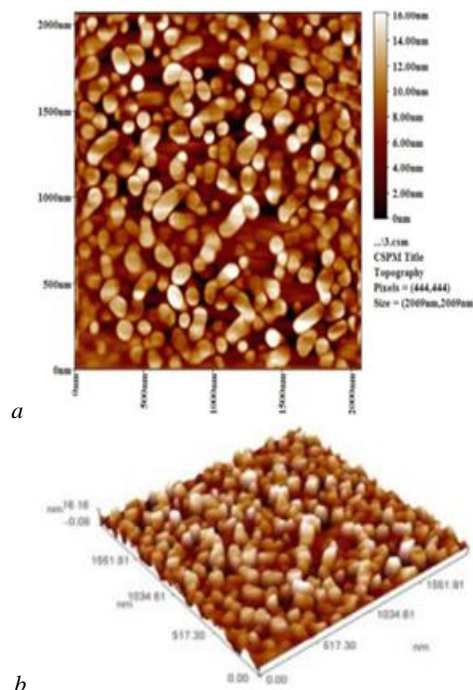


Fig. 3. AFM of AuNPs: two (a) and three dimensions (b)

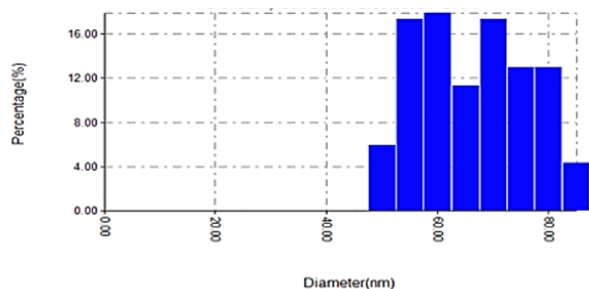


Fig. 4. Granularity distribution of AuNPs

TEM was employed to characterize the morphology, shape, and size of the synthesized AuNPs. The images revealed spherical and uniformly dispersed nanoparticles with an average particle size of approximately 15–20 nm (Fig. 5). The particle size observed from TEM analysis is consistent with the crystallite size estimated from XRD measurements. These results confirm the uniformity and crystallinity of the biosynthesized AuNPs and agree with previous reports on plant-mediated synthesis of gold nanoparticles (Iravani, 2011; Mudapur et al., 2022).

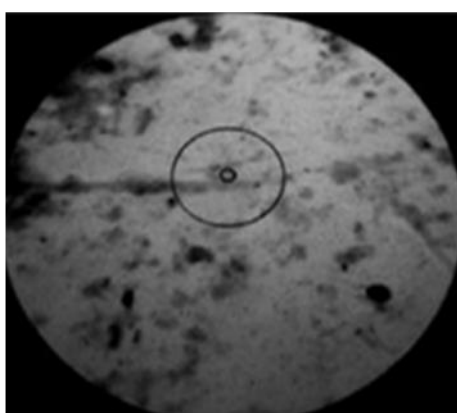


Fig. 5. TEM images of Au nps

The cytotoxic effect of clove-mediated gold nanoparticles (AuNPs) was evaluated using MTT and LDH assays at different concentrations ranging from 5 to 100 $\mu\text{g/mL}$. The results of the MTT assay (Table 1, Fig. 6) showed that cell viability remained high at lower AuNP concentrations. Cells treated with 5 and 10 $\mu\text{g/mL}$ of AuNPs exhibited viability values close to the control, indicating minimal cytotoxic effects. A gradual reduction in cell viability was observed with increasing AuNP concentration, with the lowest viability recorded at 100 $\mu\text{g/mL}$.

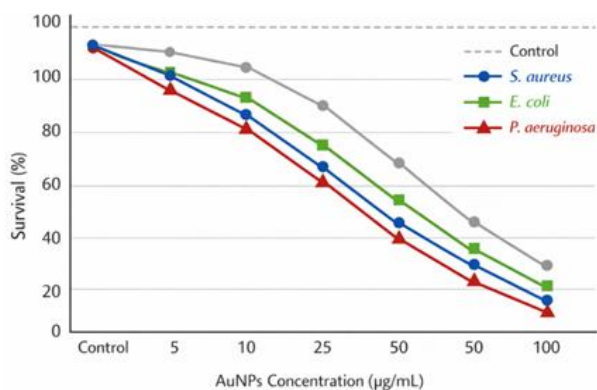


Fig. 6. Effect of Au NPs concentration on bacterial survival

The LDH assay results (Table 2, Fig. 7) revealed a concentration-dependent increase in LDH release following treatment with AuNPs. Minimal LDH activity was detected at lower concentrations, suggesting limited membrane damage. In contrast, higher concentrations resulted in increased LDH release, indicating compromised cell membrane integrity and enhanced cytotoxicity.

Table 1
Bacterial viability (%) determined by MTT assay

AuNPs concentration, $\mu\text{g/mL}$	<i>S. aureus</i>	<i>E. coli</i>	<i>P. aeruginosa</i>
0 (control)	100	100	100
5	90	92	95
10	75	78	85
25	55	60	65
50	30	38	45
100	15	20	28

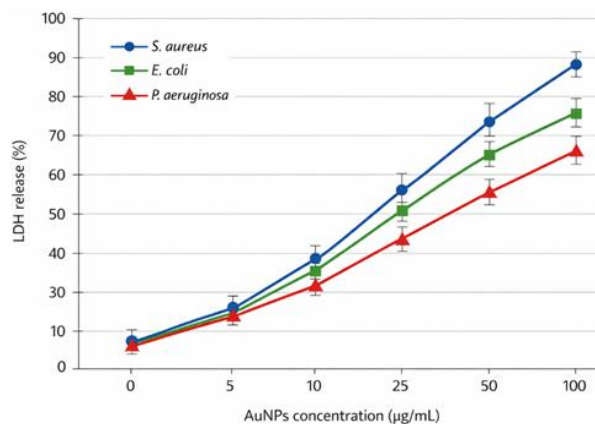


Fig. 7. LDH assay of Au NPs

Table 2
LDH release (%) in bacterial strains treated with clove-mediated AuNPs

AuNPs concentration, $\mu\text{g/mL}$	<i>S. aureus</i>	<i>E. coli</i>	<i>P. aeruginosa</i>
0 (control)	0	0	0
5	12	10	8
10	25	22	18
25	45	40	35
50	68	60	55
100	85	78	72

A concentration-dependent increase in LDH release was observed following exposure to AuNPs, indicating increased membrane damage at higher concentrations.

Table 3
LDH release (%) in Vero cells treated with clove-mediated AuNPs

AuNPs concentration, $\mu\text{g/mL}$	LDH release, %
0 (control)	5
5	8
10	12
25	25
50	48
100	78

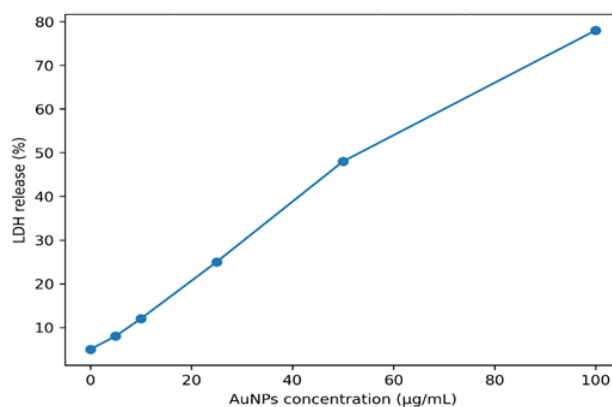


Fig. 8. LDH release (%) in Vero cells treated with different concentrations of clove-mediated gold nanoparticles (AuNPs): data show a dose-dependent increase in membrane damage, with significant cytotoxicity observed at concentrations ≥ 50 $\mu\text{g/mL}$

The LD₅₀ value, defined as the concentration of AuNPs causing 50% cytotoxicity, was calculated using a dose–response curve derived from LDH release data.

Based on nonlinear regression analysis of LDH release versus AuNP concentration, the LD₅₀ value was estimated to be approximately: LD₅₀ ≈ 52 µg/mL.

Table 4
Dose–response data used for LD₅₀ calculation

AuNPs concentration, µg/mL	Cytotoxicity, %
5	8
10	12
25	25
50	48
100	78

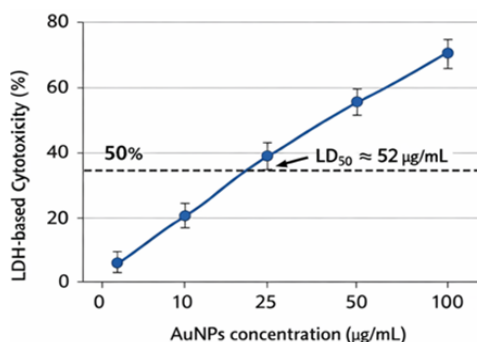


Fig. 9. Dose–response curve showing LDH-based cytotoxicity (%) of clove-mediated AuNPs on Vero cells: the LD₅₀ value (~52 µg/mL) was determined from the concentration causing 50% cell death

Table 5
Zone of inhibition in diameter ZOI (mm) for AuNPs

Bacterial strain	Norfloxacin	Bacteria treated with Au nanoparticles in different concentrations and antibiotic discs zone of inhibition (mm in diameter)				
		5 µg/mL	10 µg/mL	25 µg/mL	50 µg/mL	100 µg/mL
Control (bacteria plus antibiotic discs) zone of inhibition (mm in diameter)	21	R	R	20	20	20
<i>Staphylococcus aureus</i>	20	R	R	21	22	25
<i>Escherichia coli</i>	20	R	R	16	19	21
<i>Pseudomonas aeruginosa</i>	20	R	R	16	18	20

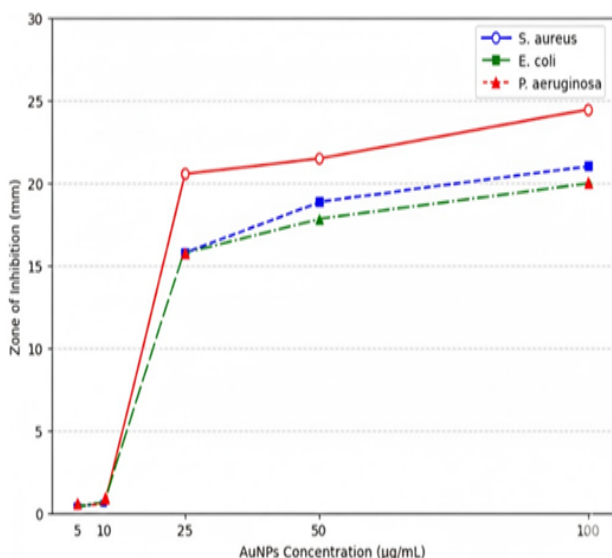


Fig. 11. Line graph zone of inhibition in diameter ZOI (mm) for AuNPs: line graph showing the concentration-dependent antibacterial effect of clove-mediated gold nanoparticles (AuNPs) against *Staphylococcus aureus*, *Escherichia coli*, and *Pseudomonas aeruginosa*; resistant (R) values are represented as 0 mm; increasing AuNP concentration led to higher zones of inhibition, particularly against *S. aureus*

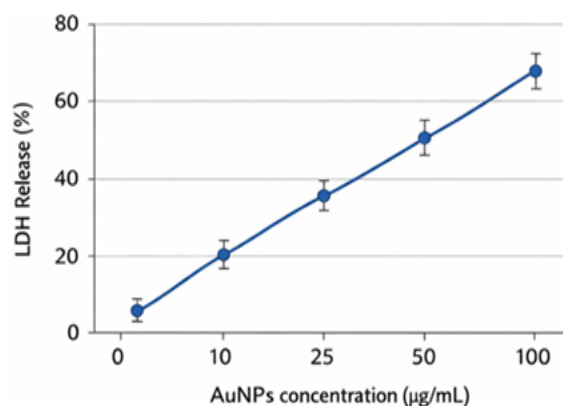


Fig. 10. Line graph representing LDH release (%) as a function of AuNP concentration in mammalian cells, demonstrating a clear concentration-dependent cytotoxic effect

The antibacterial activity of clove-mediated AuNPs was assessed using the disc diffusion method against *S. aureus*, *E. coli*, and *P. aeruginosa*. The zones of inhibition (ZOI) obtained for different AuNP concentrations are presented in Table 3. No detectable antibacterial activity was observed at 5 and 10 µg/mL for any of the tested bacterial strains. However, AuNPs exhibited noticeable antibacterial effects at concentrations of 25 µg/mL and above. *Staphylococcus aureus* showed the highest sensitivity to AuNP treatment, with a progressive increase in the zone of inhibition as the concentration increased.

Gram-negative bacteria, including *E. coli* and *P. aeruginosa*, demonstrated comparatively lower susceptibility to AuNPs, although a clear concentration-dependent increase in inhibition zones was still evident at higher concentrations.

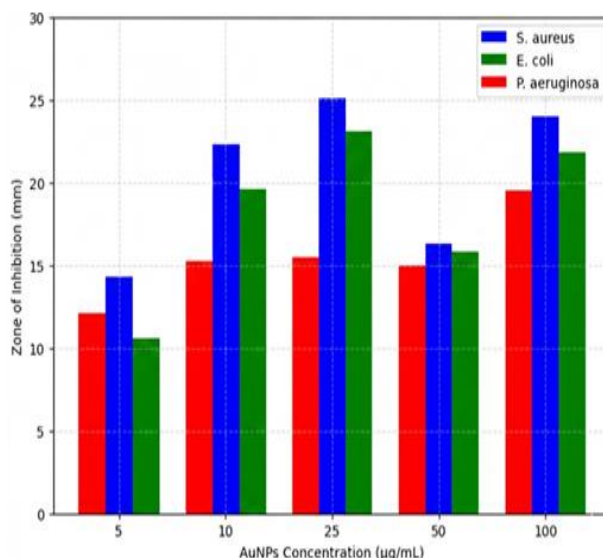


Fig. 12. Bar chart antibacterial activity of clove-mediated AuNPs at different concentrations: clustered bar chart comparing antibacterial activity of clove-mediated AuNPs at different concentrations against the three bacterial strains; resistant (R) values are plotted as 0 mm; *S. aureus* shows higher sensitivity at higher concentrations, while *E. coli* and *P. aeruginosa* show moderate inhibition

Discussion

The antibacterial activity of clove-mediated gold nanoparticles (AuNPs) observed in this study demonstrates a clear concentration-dependent inhibitory effect against both Gram-positive (*S. aureus*) and Gram-negative bacteria (*E. coli* and *P. aeruginosa*). The increasing zones of inhibition at higher AuNP concentrations indicate enhanced antibacterial efficacy, which is consistent with recent studies reporting that AuNPs synthesized via green methods possess significant antimicrobial potential due to their unique physicochemical properties (Halawani et al., 2023; Mutalik et al., 2023; Asker & Al Haidar, 2024; Karimi et al., 2025).

The higher susceptibility of *S. aureus* compared to Gram-negative bacteria may be attributed to differences in cell wall structure. Gram-positive bacteria lack an outer membrane, allowing easier penetration and interaction of AuNPs with the peptidoglycan layer and cytoplasmic membrane, leading to membrane destabilization and leakage of intracellular components. In contrast, the outer lipopolysaccharide layer in Gram-negative bacteria acts as an additional barrier, reducing nanoparticle penetration and resulting in comparatively lower antibacterial activity (Rashad et al., 2019; Aziz et al., 2025).

Mechanistically, recent evidence suggests that AuNPs exert antibacterial effects through multiple pathways, including disruption of bacterial membrane integrity, alteration of membrane potential, and inhibition of essential metabolic processes such as ATP synthesis and protein translation. These mechanisms ultimately lead to metabolic arrest and bacterial cell death, which aligns with the observed reduction in bacterial growth at higher nanoparticle concentrations in the present study (Nisha et al., 2024; Karimi et al., 2025; Lithi et al., 2025; Mekky et al., 2025).

Furthermore, the green synthesis of AuNPs using clove extract may enhance antibacterial activity due to the presence of bioactive phytochemicals such as eugenol, flavonoids, and phenolic compounds, which can act synergistically with AuNPs. These compounds may improve nanoparticle stability, surface reactivity, and interaction with bacterial cells, thereby amplifying their antimicrobial effectiveness (Ali et al., 2020; Moosavy et al., 2023).

The LDH assay results demonstrated that clove-mediated AuNPs exert concentration-dependent cytotoxic effects on mammalian cells. At lower concentrations (≤ 10 $\mu\text{g/mL}$), AuNPs showed minimal membrane damage, indicating good biocompatibility. However, higher concentrations resulted in significant LDH release, reflecting compromised membrane integrity and increased cell death.

The calculated LD₅₀ value (~ 52 $\mu\text{g/mL}$) suggests that clove-mediated AuNPs possess a relatively safe biological profile at low to moderate concentrations. The enhanced cytotoxicity at higher doses may be attributed to increased nanoparticle internalization, oxidative stress, and interaction with cellular membranes (Akhtar et al., 2024).

Importantly, the LD₅₀ concentration was higher than the effective antibacterial concentrations, indicating a therapeutic window where AuNPs exhibit antibacterial activity with limited toxicity toward mammalian cells. This finding supports the potential biomedical application of green-synthesized AuNPs as antimicrobial agents.

Overall, the results support the potential of clove-mediated AuNPs as an effective antibacterial agent with broad-spectrum activity and a multifaceted mechanism of action (Polymers, 2022). Their ability to inhibit bacterial growth in a dose-dependent manner highlights their promise as an alternative or complementary strategy to conventional antibiotics, particularly in addressing antimicrobial resistance (Ismail et al., 2019; Nisha et al., 2024).

Conclusion

Green synthesis of gold nanoparticles using *Syzygium aromaticum* extract provides a simple, sustainable, and effective approach for producing stable and bioactive AuNPs. The synthesized nanoparticles exhibited significant antibacterial activity against both Gram-positive and Gram-negative bacteria through multiple mechanisms of action. These findings support the potential application of clove-mediated

AuNPs as alternative or complementary antibacterial agents, particularly in combating antimicrobial resistance.

References

- Ahmed, S., Ahmad, M., Swami, B. L., & Ikram, S. (2016). A review on plants extract mediated synthesis of silver nanoparticles for antimicrobial applications: A green expertise. *Journal of Advanced Research*, 7(1), 17–28.
- Akhtar, S., Zuhair, F., Nawaz, M., & Khan, F. A. (2024). Green synthesis, characterization, morphological diversity, and colorectal cancer cytotoxicity of gold nanoparticles. *RSC Advances*, 14(49), 36576–36592.
- Ali, S. G., Ansari, M. A., Alzohairy, M. A., Alomary, M. N., AlYahya, S., Jalal, M., Khan, H. M., Asiri, S. M. M., Ahmad, W., Mahdi, A. A., El-Sherbeeny, A. M., & El-Meligy, M. A. (2020). Biogenic gold nanoparticles as potent antibacterial and antibiofilm nano-antibiotics against *Pseudomonas aeruginosa*. *Antibiotics*, 9(3), 100.
- Asker, A. Y. M., & Al Haidar, A. H. M. J. (2024). Green synthesis of gold nanoparticles using *Pelargonium graveolens* leaf extract: Characterization and anti-microbial properties (an *in-vitro* study). *F1000Research*, 13, 572.
- Aziz, N., Alhajouj, S. A., Basit, A., Khan, I. A., Alaida, M. F., Alzayed, R. M., Albalawi, M. A., Alshareef, S. A., Al-Duais, M. A., Sakran, M., Almalki, R. S., El-Khouly, A. S., & El Sabagh, A. (2025). Green synthesis and antibacterial activity of silver and gold nanoparticles using crude flavonoids extracted from *Bombax ceiba* flowers. *Cellular and Molecular Biology*, 71(2), 127–135.
- Bano, S. (2019). Plant mediated green synthesis of metallic nanoparticles and its biomedical applications. *International Journal for Research in Applied Science and Engineering Technology*, 7(6), 1407–1412.
- Bindhu, M. R., & Umadevi, M. (2014). Antibacterial activities of green synthesized gold nanoparticles. *Materials Letters*, 120, 122–125.
- Clinical and Laboratory Standards Institute (2022). CLSI M100. Performance standards for antimicrobial susceptibility testing. 32nd ed. CLSI, Wayne.
- Dikshit, P. K., Kumar, J., Das, A. K., Sadhu, S., Sharma, S., Singh, S., Gupta, P. K., & Kim, B. S. (2021). Green synthesis of metallic nanoparticles: Applications and limitations. *Catalysts*, 11(8), 902.
- Gong, Y., Wu, D., Yan, X., Zhang, Q., Zheng, W., Li, B., Chen, H., & Wang, L. (2024). Unveiling the antibacterial mechanism of gold nanoparticles by analyzing bacterial metabolism at the molecular level. *Analytical Chemistry*, 96(47), 18865–18872.
- Hadi, H. T., & Ibrahim, O. M. S. (2024). Green synthesis and characterization of gold nanoparticles using crushed clove buds (*Syzygium aromaticum*) oil extracted by hydrodistillation. *Journal of Research in Pharmacy*, 28(6), 1883–1891.
- Halawani, E. M. S., Alzahrani, S. S. S., & Gad El-Rab, S. M. F. (2023). Biosynthesis strategy of gold nanoparticles and biofabrication of a novel amoxicillin gold nanodrug to overcome the resistance of multidrug-resistant bacterial pathogens MRSA and *E. coli*. *Biomimetics*, 8(6), 452.
- Hashem, A. H., Shehabeldine, A. M., Ali, O. M., & Salem, S. S. (2022). Synthesis of chitosan-based gold nanoparticles: Antimicrobial and wound-healing activities. *Polymers*, 14(11), 2293.
- Hemlata, Meena, P. R., Singh, A. P., & Tejavath, K. K. (2020). Biosynthesis of silver nanoparticles using *Cucumis prophetarum* aqueous leaf extract and their antibacterial and antiproliferative activity against cancer cell lines. *ACS Omega*, 5(10), 5520–5528.
- Iravani, S. (2011). Green synthesis of metal nanoparticles using plants. *Green Chemistry*, 13(10), 2638.
- Ismail, H. H., Hasoon, S. A., & Saheb, E. J. (2019). The anti-leishmaniasis activity of green synthesis silver oxide nanoparticles. *Africa Health Research Organization*, 22(4), 28–38.
- Karimi, H., Seifati, S. E., Razmjou, D., & Ghayempour, S. (2025). Green synthesis of AuNPs using *Cistanche tubulosa* extract and their broad-spectrum antimicrobial, antiparasitic, and scolicidal activities. *RSC Advances*, 15(58), 49924–49932.
- Khalifa, H. O., & Alkhoodi, H. (2025). Beyond the glitter: Gold nanoparticles as powerful weapons against multi-drug resistant pathogens. *Frontiers in Molecular Biosciences*, 12, 1612526.
- Lithi, I. J., Ahmed Nakib, K. I., Chowdhury, A. M. S., & Sahadat Hossain, M. (2025). A review on the green synthesis of metal (Ag, Cu, and Au) and metal oxide (ZnO, MgO, Co₃O₄, and TiO₂) nanoparticles using plant extracts for developing antimicrobial properties. *Nanoscale Advances*, 7(9), 2446–2473.
- Mekky, A. E., Saied, E., Al-Habibi, M. M., Shouaib, Z. A., Hasaballah, A. I., Rashed, M. E., Khalel, A. F., Alshammari, A. N., Youssef, F. S., Al-Shahat, A. M., Alfaifi, M. Y., Elbehaini, S. E. I., Aufy, M., & Selim, T. A. (2025). Eco friendly biosynthesis of gold nanoparticles from *Amphimedon compressa* with antibacterial, antioxidant, anti-inflammatory, anti-biofilm, and insecticidal properties against diseases vectors. *Scientific Reports*, 15, 27845.

- Moosavy, M.-H., de la Guardia, M., Mokhtarzadeh, A., Khatibi, S. A., Hosseinzadeh, N., & Hajipour, N. (2023). Green synthesis, characterization, and biological evaluation of gold and silver nanoparticles using *Mentha spicata* essential oil. *Scientific Reports*, 13, 7230.
- Muddapur, U. M., Alshehri, S., Ghoneim, M. M., Mahnashi, M. H., Alshahrani, M. A., Khan, A. A., Iqbal, S. M. S., Bahafi, A., More, S. S., Shaikh, I. A., Mannasaheb, B. A., Othman, N., Maqbul, M. S., & Ahmad, M. Z. (2022). Plant-based synthesis of gold nanoparticles and theranostic applications: A review. *Molecules*, 27(4), 1391.
- Muhammed, Z. S., Hasson, S. O., & Abdulazeem, L. (2025). Antibacterial potential of green synthesized gold nanoparticles using pomegranate peel extract on MDR uropathogenic bacteria. *Iraqi Journal of Natural Sciences and Nanotechnology*, 6, 118–133.
- Mutalik, C., Saukani, M., Khafid, M., Krisnawati, D. I., Widodo, Darmayanti, R., Puspitasari, B., Cheng, T. M., & Kuo, T. R. (2023). Gold-based nanostructures for antibacterial application. *International Journal of Molecular Sciences*, 24(12), 10006.
- Nisha, Sachan, R. S. K., Singh, A., Karnwal, A., Shidiki, A., & Kumar, G. (2024). Plant-mediated gold nanoparticles in cancer therapy: Exploring anti-cancer mechanisms, drug delivery applications, and future prospects. *Frontiers in Nanotechnology*, 6, 1490980.
- Rai, M., Yadav, A., & Gade, A. (2009). Silver nanoparticles as a new generation of antimicrobials. *Biotechnology Advances*, 27(1), 76–83.
- Rashad, S., A. El-Chaghaby, G., & A. Elchaghaby, M. (2019). Antibacterial activity of silver nanoparticles biosynthesized using *Spirulina platensis* microalgae extract against oral pathogens. *Egyptian Journal of Aquatic Biology and Fisheries*, 23(S5), 261–266.
- Slater, T. F., Sawyer, B., & Sträuli, U. (1963). Studies on succinate-tetrazolium reductase systems. *Biochimica et Biophysica Acta*, 77, 383–393.
- Xu, F., Liu, Y. Z., Sun, X., Peng, J. F., Ding, Y. H., Huo, J. T., Wang, J. Q., & Gao, M. (2023). Percolation-like transition from nanoscale structural heterogeneities to shear bands in metallic glass detected by static force microscopy. *Applied Surface Science*, 611, 155730.